Accuracy Analysis of Sensing Coils in 2-D Magnetic Properties Measurement

Xiaofeng Ding and Suping Ren

School of Automation Science and Electrical Engineering, Beihang University, Beijing 100191, China

There has been an increasing awareness of research on magnetic properties of soft magnetic materials. In reality, the soft magnetic materials are likely to be magnetized by 2-D rotating magnetic field. Moreover, the magnetic properties could be influenced by mechanical stress. In order to investigate the magnetic properties thoroughly, numerous measurement apparatuses have been developed, which could take rotating magnetic flux or mechanical stress into account. However, there is limited research on the investigation of 2-D magnetic properties affected by laminated direction mechanical stress, as few mature devices could be employed, since the traditional B–H sensing coils are easily damaged by laminated direction stress. Therefore, the sensing structure with cubic specimen is proposed for 2-D magnetic properties measurement considering laminated direction stress. The printed circuit board (PCB)-based B–H sensing coils, which are attached to the surrounding surface of the cubic specimen, could be free of the impact of the z-direction mechanical stress. The accuracy of B–H sensing part is analyzed in detail by means of the finite-element method as well as experiments. And, more remarkable, the deficiency of the artificial H-coils wound by enameled wire is presented. Hence, a modified H-coil made of four layer PCBs is proposed in this paper, the measurement accuracy is proven through experiments.

Index Terms—**2-D magnetic properties, B–H sensing coils, finite-element method (FEM), soft magnetic materials.**

I. Introduction

IT HAS long been recognized that the rotating magnetic flux appears in electrical machine cores and leads to considerable power loss [1]. As motor efficiency concerned, the rotating magnetic properties of electrical steel sheets need to be investigated thoroughly, and the rotating power loss requires accurate prediction. As a consequence, a substantial body of the literature has been undertaken on the measurement of 2-D vector magnetic properties.

The rotational single sheet tester (RSST) was proposed to examine the comprehensive magnetic properties of square electrical steel sheet, including the properties under alternating magnetization along arbitrary direction and the properties under rotating magnetization [2]. In order to enhance the induction levels of tested square specimen magnetized by small magnetomotive force, the RSST is modified. The vertical–horizontal "double-C" yoke structure is employed, and the air gap between the specimen and exciting pole is minimized [3]. However, the magnetic field in square specimen presents inhomogeneity due to demagnetizing effect. Meanwhile, the strong magnetic field could be hardly achieved at high frequency [4]. Thus, a novel broadband three-phase magnetizer apparatus with circular specimen is developed, which could overcome the drawbacks [5].

In addition, the magnetic properties of electrical steel sheet are affected by stress because of produce process and external environment. The alternating magnetic properties influenced by laminated direction stress as well as magnetization direction stress have been explored, by applying specific apparatuses [6]–[9]. Furthermore, a novel 2-D magnetic properties tester considering mechanical stress was developed. The tester is based on cross-specimen, and investigates the 2-D magnetic properties of specimen under stresses along two magnetization directions [10]. Nevertheless, there is a lack of research on 2-D magnetic properties of electrical steel sheet under laminated direction stress, and a few mature measurement apparatus have been proposed.

Meanwhile, in most 2-D magnetic properties measurement, vectors $\boldsymbol{B}$ (magnetic flux density) and $\boldsymbol{H}$ (magnetic field strength) are detected by $\boldsymbol{B}$-coils wound in two micro-holes drilled on specimen and $\boldsymbol{H}$-coils attached to specimen tightly [11]. Both $\boldsymbol{B}$-coils and $\boldsymbol{H}$-coils are utilized according to the law of electromagnetic induction.

Recently, the needle probe method is reported to measure $\boldsymbol{B}$, based on the potential difference produced by eddy current in tested specimen [12]. However, in the 2-D magnetic properties measurement considering laminated direction stress, the traditional micro-holes method, novel needle probe method, and $\boldsymbol{H}$-coils could not be employed, since $\boldsymbol{B}$- and $\boldsymbol{H}$-sensing parts are restricted to destruction due to laminated direction mechanical stress. While a novel sensing structure with cubic specimen is designed for 3-D magnetic properties measurement [13]. The sensing structure could be expanded to 2-D property measurement considering laminated direction stress, as all the sensing coils attached to the specimen surfaces which is parallel to the stress direction, whereas the accuracy of the novel sensing has not been emphasized.

Therefore, in this paper, the sensing structure with cubic specimen is utilized to 2-D properties measurement considering laminated direction stress. The sensing coils are designed based on printed circuit board (PCB), which could improve the reliability and accuracy of B–H sensing part. The accuracy of the sensing structure proposed in this paper is analyzed in detail by applying the finite-element method (FEM), and validated by experiments.

II. 2-D Magnetic Properties Measuring Apparatus

The 2-D magnetic properties measuring apparatus considered the laminated direction mechanical stress is illustrated

Manuscript received March 16, 2018; revised April 23, 2018; accepted May 12, 2018. Date of publication July 25, 2018; date of current version October 17, 2018. Corresponding author: S. Ren (e-mail: rsp93_4@126.com).

Color versions of one or more of the figures in this paper are available online at http://ieeexplore.ieee.org.

Digital Object Identifier 10.1109/TMAG.2018.2839748

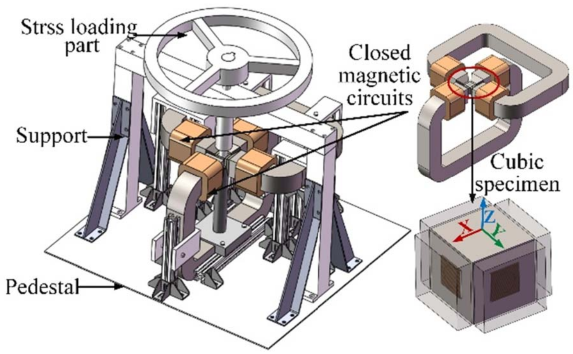

Fig. 1. 2-D magnetic properties measuring apparatus.

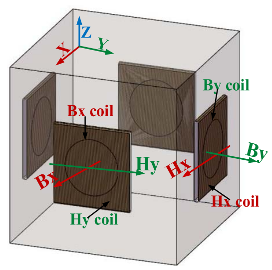

Fig. 2. Structure of B and H sensing coils.

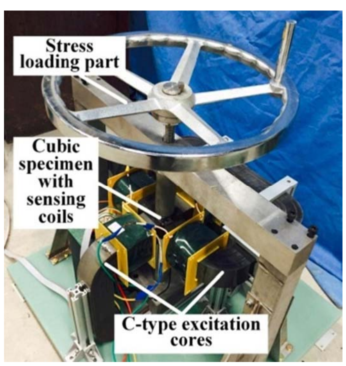

Fig. 3. Photograph of the real setup.

in Fig. 1. The overall apparatus is composed of stress loading part, closed magnetic circuits, support, and pedestal. The closed magnetic circuits consists of two orthogonal "C-type" yokes, exciting coils and cubic specimen with four surrounding core shoes. As the amplitude, frequency, and phase of the x- and y-direction currents are controlled, vector $\boldsymbol{B}$ along the arbitrary direction in magnetization xoy plane could be induced in the specimen. And the stress along the z-direction, which is parallel to laminated direction of electrical steel sheets specimen, is exerted by rotating the handle wheel.

The sensing coils for $\boldsymbol{B}$ and $\boldsymbol{H}_x$ are attached to the surfaces of the cubic specimen, as shown in Fig. 2. And $\boldsymbol{B}$ or $\boldsymbol{H}$ coils fixed on the opposite surfaces are connected in series. Thus, B_x- and B_y-coils detect the x- and y-direction components of $\boldsymbol{B}$ in specimen, respectively. In the meantime, according to the boundary condition of magnetic field strength, H_x- and H_y-coils detect the x- and y-direction components of $\boldsymbol{H}$ on the surface of specimen. The photograph of the real setup is shown in Fig. 3.

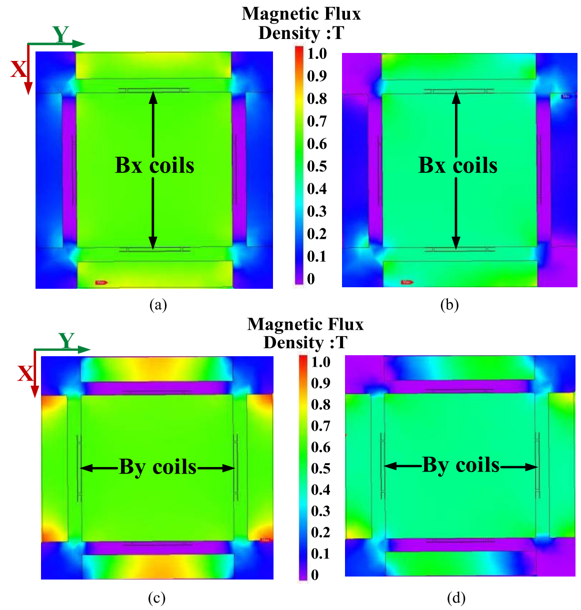

Fig. 4. Distribution of B_x and B_y components in specimen and B sensing coils regions. (a) $B_x = 0.6$ T. (b) $B_x = 0.4$ T. (c) $B_y = 0.6$ T. (d) $B_y = 0.4$ T.

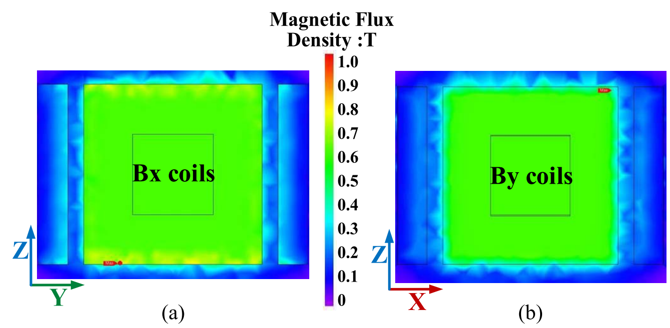

Fig. 5. Distribution of B_x and B_y components within B sensing coils regions. (a) $B_x = 0.6$ T. (b) $B_y = 0.6$ T.

III. Accuracy Analysis of B and H Sensing Coils

In the measurement of 2-D magnetic properties of electrical steel sheet, there is a great concern on the accuracy of sensing structure for $\boldsymbol{B}$ and $\boldsymbol{H}$. In this section, the accuracy of the sensing coils in the apparatus is validated by both FEM and experiments. The structure of $\boldsymbol{B}$-coils and modified H-coils are described in detail, and the calibration of $\boldsymbol{B}$-coils and modified H-coils are presented.

A. FEM Analysis of Closed Magnetic Circuit

In the FEM analysis of closed magnetic circuits, the currents which present 5 A amplitude, 50 Hz frequency, and 90° phase difference are set to the exciting coils. The distribution of B_x and B_y components both in specimen and $\boldsymbol{B}$ sensing coils regions are shown in Fig. 4. Each component of vector $\boldsymbol{B}$ is homogeneous in specimen, and equal to the counterpart in $\boldsymbol{B}$ sensing coils regions. Besides, on the surface which $\boldsymbol{B}$ sensing coils attached to, the magnetic flux density distributions are displayed in Fig. 5. B_x and B_y components present homogeneous within $\boldsymbol{B}$ sensing coils regions.

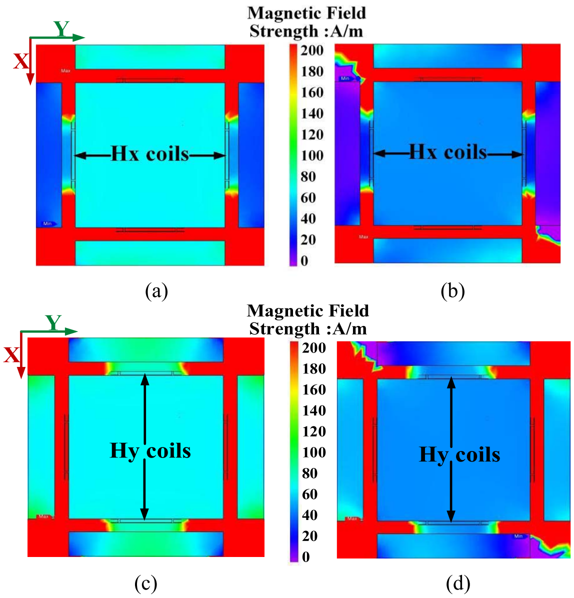

Fig. 6. Distribution of H_x and H_y components in specimen and H sensing coils regions. (a) $B_x = 0.6$ T. (b) $B_x = 0.4$ T. (c) $B_y = 0.6$ T. (d) $B_y = 0.4$ T.

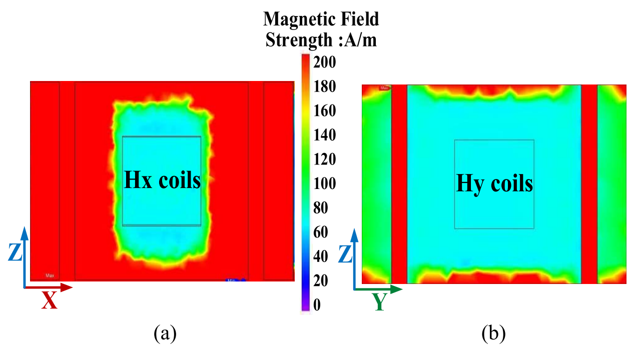

Fig. 7. Distribution of H_x and H_y components within H sensing coils regions. (a) $B_x = 0.6$ T. (b) $B_y = 0.6$ T.

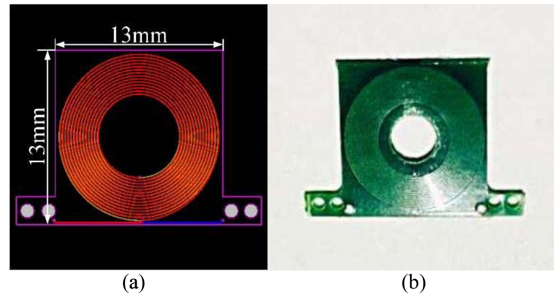

Fig. 8. B sensing coils. (a) PCB diagram. (b) Product.

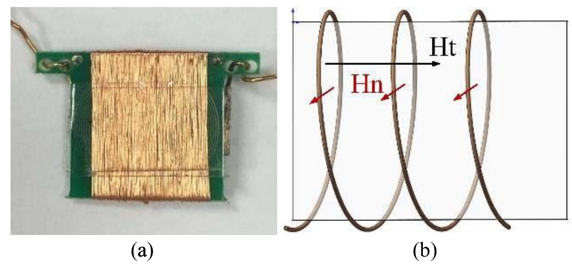

Fig. 9. Original H sensing coils. (a) Product. (b) Magnetic field strength that the H sensing coils detected.

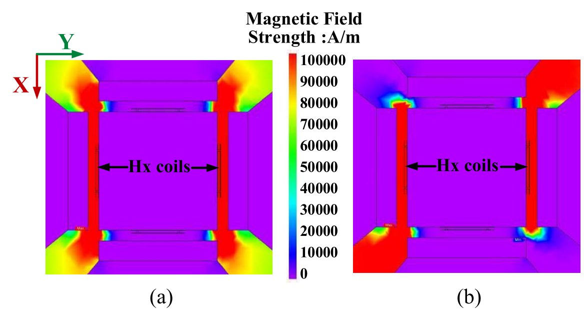

Fig. 10. Distribution of H_y components within H_x-coils regions. (a) $B_y = 0.6$ T. (b) $B_y = 0.4$ T.

In the same way, H_x and H_y components in specimen and ***H*** sensing coils regions are also examined. Fig. 6 shows H_x and H_y components in specimen and ***H*** sensing coils regions. It indicates that each component of ***H*** in specimen is homogeneous, and the same as the counterpart in ***H*** sensing coils regions. Furthermore, on the surfaces of specimen, H_x and H_y distribution is homogeneous within the regions of H_x- and H_y-coils, as illustrated in Fig. 7

B. Structure of B and H Sensing Coils

In the 2-D magnetic properties measuring apparatus, all ***B*** and ***H*** sensing coils are maintained in the gap which locates between cubic specimen and core shoes. As a consequence, small thickness of sensing coils is preferred to enhance the magnetic field induced in specimen and improve the measuring accuracy. Hence, ***B***-coils made of four-layer PCBs are employed, as presented in Fig. 8. The thickness of the PCB for ***B***-coil is less than 1 mm.

In addition, the original ***H*** sensing coils are wound around the PCB of ***B***-coils, as displayed in Fig. 9(a).The manual ***H***-coils are not ideal, as there is equivalent closed loop whose area is perpendicular to H_n (the normal component of magnetic field strength), as shown in Fig. 9(b). Thus, the original ***H***-coils detect both H_t (the tangential component of magnetic field strength) and H_n. However, in the measurement of 2-D magnetic properties, H_n in sensing coils regions is considerable. It can be observed from Fig. 10, the normal component H_y within the regions of H_x-coils is greater than 100 000 A/m, while the tangential component H_x is less than 100 A/m, as shown in Fig. 6(a). Hence, the excess induced voltage of ***H***-coils is acquired, and the value of ***H*** could not be obtained accurately.

A modified ***H***-coil made of four layer PCBs proposed in this paper. Fig. 11 shows the PCB diagram as well as the product of modified ***H***-coils. The conductors arranged on the top and bottom layers constitute 25 turns closed conductors, and the conductors on the two middle layers compose 25 turns closed conductors. Since the projection of the conductors of each coil is coincided perfectly, the equivalent closed loop whose area is perpendicular to H_n is eliminated. Consequently, the modified ***H***-coils just examine the tangential component of ***H*** on the boundary which is between the specimen and gap. The thickness of ***H*** sensing coil is 1 mm, and the thickness of

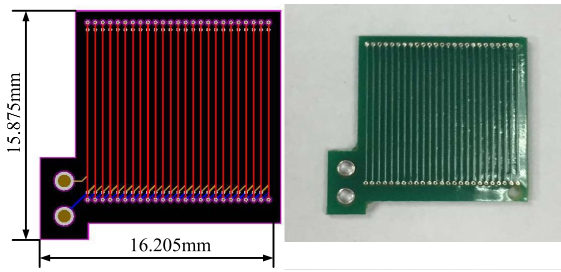

(a) (b)

Fig. 11. Modified H sensing coils. (a) PCB diagram. (b) Product.

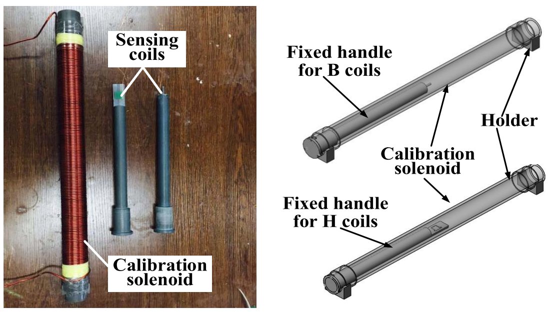

(a) (b)

Fig. 12. Calibration solenoid. (a) Prototype of the solenoid. (b) Structure of the solenoid with two fixed handles for H and B coils, respectively.

the overall sensing structure for $\boldsymbol{B}$ and $\boldsymbol{H}$ is less than 2 mm. In the previous FEM analysis of measuring apparatus, the gap between core shoes and specimen is 2 mm. The tangential component of $\boldsymbol{H}$ is homogeneous within the sensing structure region, and equal to the counterpart in specimen. Therefore, the precision of modified $\boldsymbol{H}$ sensing coils is verified.

C. Calibration of B and H Sensing Coils

In order to calculate $\boldsymbol{B}$ and $\boldsymbol{H}$ of specimen precisely based on the induced voltage of sensing coils, there is an urgent demand for the exact correspondence relationship between the voltage of sensing coils and the value of $\boldsymbol{B}$ and $\boldsymbol{H}$. The correspondence could be expressed in the following equation:

$$\begin{cases} B_i = -K_{\mathrm{BV}} \int V_{\mathrm{Bi}} dt, & (i = x, y) \\ H_i = -K_{\mathrm{HV}} \int V_{\mathrm{Hi}} dt, & (i = x, y) \end{cases} \tag{1}$$

where V_{Bi} and V_{Hi} are the induced voltages of sensing coils, K_{BV} and K_{HV} are the coefficients obtained by calibration. The calibration apparatus is illustrated in Fig. 12. The standard magnetic field is generated in the center of solenoid, when the sinusoidal current is set to the exciting coils. In accordance with the voltage of sensing coils, the calibration coefficients are gained: $K_{\mathrm{BV}} = 122.33$ and $K_{\mathrm{HV}} = 1.48 \times 109$.

IV. Experimental Analysis

For further validation of $\boldsymbol{B}$ and $\boldsymbol{H}$ sensing structure in 2-D magnetic properties measurement, the experiments measuring $\boldsymbol{B}$ and $\boldsymbol{H}$ in tested specimen are conducted. Meanwhile, the experimental results applied original $\boldsymbol{H}$-coils and modified $\boldsymbol{H}$-coils are compared and analyzed.

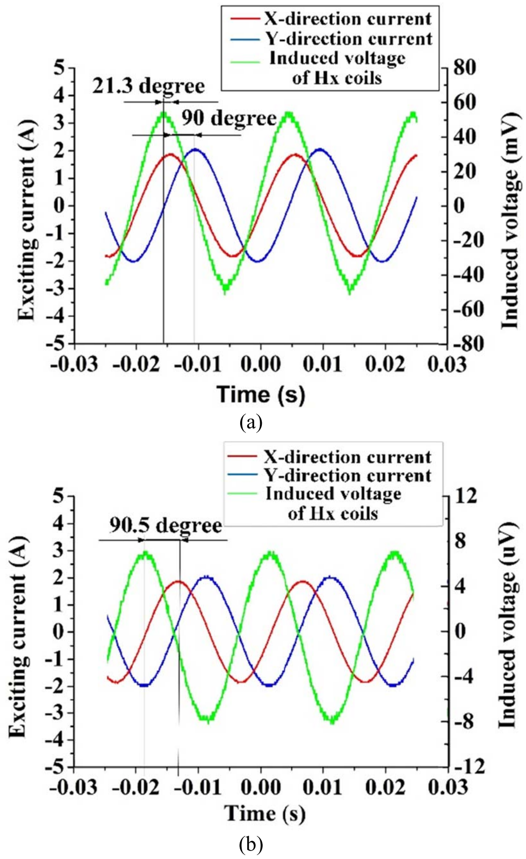

Fig. 13. Two directions exciting currents and the induced voltage of H_x-coils. (a) Results of original H_x-coils. (b) Results of modified H_x-coils.

A. Experimental Comparison Between Original H-Coils and Modified H-Coils

The magnetic property of tested specimen laminated by 20WTG1500 along the x-direction is examined, when two sinusoidal currents presented in Fig. 12 are set to the x- and y-direction exciting coils simultaneously. The currents present 90° difference, and lead to rotating magnetic field in tested specimen. The induced voltages of both original H_x-coils and modified H_x-coils are obtained.

According to the law of electromagnetic induction, the phase of H_x-coils induced voltage is 90° ahead of the phase of magnetic flux along the x-direction. As the exciting current shows the same phase of magnetic field in the gap, the phase of H_x-coils induced voltage presents 90° ahead of the x-direction exciting current. However, the phase difference of the original H_x-coils induced voltage and the x-direction current is 21.3°, as shown in Fig. 13(a). The obtained voltage of original H_x-coils contains considerable induced voltage which is influenced by the y-direction current. Fig. 13(b) shows the induced voltage of modified H_x-coils. The phase difference between the x-direction current and induced voltage is 90°. Besides, the component H_y is greater than H_x within the region of H_x-coils, as previously analyzed by FEM. The amplitude of original H_x-coils induced voltage is 1000 times greater than the counterpart of modified H_x-coils induced voltage. Thus, the modified H_x-coils will not be affected by the magnetic field along the y-direction.

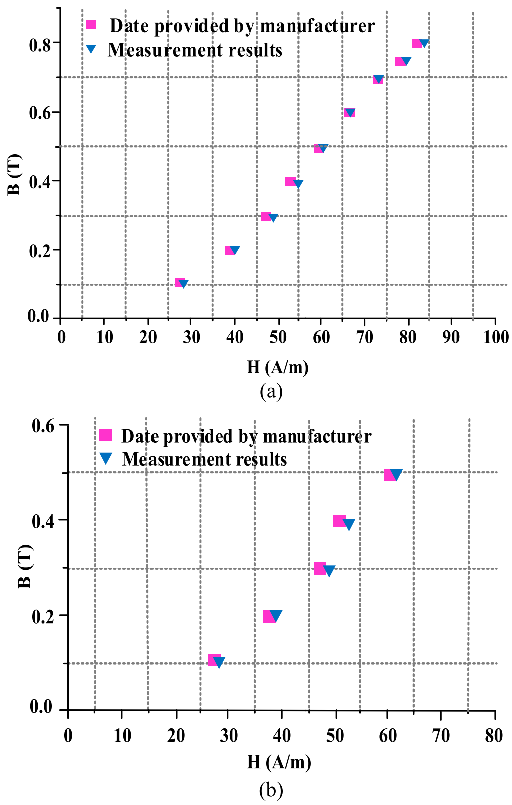

Fig. 14. *B–H* fundamental magnetization curves along the x-direction of non-oriented electrical steel. (a) Data provided by manufacturer. (b) Measurement results.

B. Measurement Results of Fundamental Magnetization Curves

For further validation of $\boldsymbol{B}$ and $\boldsymbol{H}$ sensing part, *B–H* fundamental magnetization curves along the x-direction of non-oriented electrical steel 20WTG1500 is obtained by the measurement apparatus, when magnetized by the magnetic field with different frequencies. And the measuring results are compared with the fundamental magnetization curves provided by manufacturer, which is gained by the Epstein frame measuring system, as shown in Fig. 14.

The comparison of the fundamental magnetization curves provided by manufacturer and measurement results when the frequency of magnetic field is 50 and 100 Hz are presented in Fig. 14(a) and (b), respectively. The measurement results approximate the data of manufacturer well. As for the same magnetic flux density, the magnetic field strength of measurement results is greater than the counterpart of the data of manufacturer.

V. Conclusion

In this paper, *B–H* sensing structure with cubic specimen is developed for the magnetic properties measurement which could consider 2-D rotating flux and laminated direction mechanical stress. And the accuracy of the sensing structure is analyzed by FEM. Nevertheless, original artificial $\boldsymbol{H}$-coils could not precisely measure the magnetic field strength in specimen due to the influence of the normal component H_n. Therefore, a modified $\boldsymbol{H}$-coil based on PCB is proposed, and the projection of the conductors of each coil is coincided perfectly by specific conductor arrangement. The equivalent closed loop whose area is perpendicular to H_n of modified $\boldsymbol{H}$-coils is eliminated.

B–H fundamental magnetization curves of non-oriented electrical steel are measured by implementing the 2-D magnetic properties measurement apparatus, and the measuring results are compared with the counterpart provided by manufacturer, which are gained by Epstein frame measuring system. The measurement results show little difference with *B–H* fundamental magnetization curves provided by manufacture. At the same time, we applied this method to the measurement of the magnetic properties of the motor, and achieved good results. Consequently, *B–H* sensing coils could be adopted for precise magnetic properties measurement taking 2-D rotating flux and laminated direction mechanical stress into account.

Acknowledgment

This work was supported in part by the National Natural Science Foundation of China under Project 51407004 and in part by the Aeronautical Science Foundation of China under Grant 20162851016.

References

[1] J. G. Zhu and V. S. Ramsden, "Improved formulations for rotational core losses in rotating electrical machines," *IEEE Trans. Magn.*, vol. 34, no. 4, pp. 2234–2242, Jul. 1998.

[2] M. Enokizono, T. Suzuki, and J. D. Sievert, "Measurement of iron loss using rotational magnetic loss measurement apparatus," *IEEE Transl. J. Magn. Jpn.*, vol. 6, no. 6, pp. 508–514, Jun. 1991.

[3] L. Chen, Y. Wang, Z. Zhao, H. Zhao, C. Liu, and X. Yang, "A new magnetizer for measuring the two-dimensional magnetic properties of nanocrystalline alloys at high frequencies," *IEEE Magn. Lett.*, vol. 8, no. 99, pp. 1–5, Oct. 2017.

[4] C. Ragusa and F. Fiorillo, "A three-phase single sheet tester with digital control of flux loci based on the contraction mapping principle," *J. Magn. Magn. Mater.*, vol. 304, pp. e568–e570, Sep. 2006.

[5] O. de la Barrière, C. Appino, F. Fiorillo, M. Lécrivain, C. Ragusa, and P. Vallade, "A novel magnetizer for 2D broadband characterization of steel sheets and soft magnetic composites," *Int. J. Appl. Electromagn. Mech.*, vol. 48, nos. 2–3, pp. 239–245, 2015.

[6] D. Miyagi, K. Miki, M. Nakano, and N. Takahashi, "Influence of compressive stress on magnetic properties of laminated electrical steel sheets," *IEEE Trans. Magn.*, vol. 46, no. 2, pp. 318–321, Feb. 2010.

[7] M. Kawabe, T. Nomiyama, A. Shiozaki, M. Mimura, N. Takahashi, and M. Nakano, "Magnetic properties of particular shape specimen of nonoriented electrical steel sheet under compressive stress in thickness direction," *IEEE Trans. Magn.*, vol. 48, no. 11, pp. 3462–3465, Nov. 2012.

[8] N. Takahashi *et al.*, "Method for measuring the magnetic properties of high-density magnetic composites under compressive stress," *IEEE Trans. Magn.*, vol. 43, no. 6, pp. 2749–2751, Jun. 2007.

[9] D. Miyagi, Y. Aoki, M. Nakano, and N. Takahashi, "Effect of compressive stress in thickness direction on iron losses of nonoriented electrical steel sheet," *IEEE Trans. Magn.*, vol. 46, no. 6, pp. 2040–2043, Jun. 2010.

[10] Y. Kai, Y. Tsuchida, T. Todaka, and M. Enokizono, "Influence of stress on vector magnetic property under rotating magnetic flux conditions," *IEEE Trans. Magn.*, vol. 48, no. 4, pp. 1421–1424, Apr. 2012.

[11] S. Tumanski, "Induction coil sensors—A review," *Meas. Sci. Technol.*, vol. 12, pp. R31–R46, Jan. 2007.

[12] K. Senda, M. Ishida, K. Sato, M. Komatsubara, and T. Yamaguchi, "Localized magnetic properties in grain-oriented electrical steel measured by needle probe method," *Elect. Eng. Jpn.*, vol. 126, pp. 1–11, Mar. 1999.

[13] Y. Li, Q. Yang, J. Zhu, and Y. Guo, "Magnetic properties measurement of soft magnetic composite materials over wide range of excitation frequency," *IEEE Trans. Ind. Appl.*, vol. 48, no. 1, pp. 88–97, Jan./Feb. 2012.